

---

---

# BRAIN THEORY

---

---

SPATIO-TEMPORAL ASPECTS  
OF BRAIN FUNCTION  
A. AERTSEN / EDITOR



ELSEVIER

# BRAIN THEORY

SPATIO-TEMPORAL ASPECTS  
OF BRAIN FUNCTION

Edited by

**A. AERTSEN**

Institut für Neuroinformatik  
Rühr-Universität Bochum  
Bochum, Germany



1993

ELSEVIER

AMSTERDAM - LONDON - NEW YORK - TOKYO

ELSEVIER SCIENCE PUBLISHERS B.V.  
Sara Burgerhartstraat 25  
P.O. Box 211, 1000 AE Amsterdam, The Netherlands

ISBN: 0 444 89839 5

© 1993 Elsevier Science Publishers B.V. All rights reserved.

No part of this publication may be reproduced, stored in a retrieval system or transmitted in any form or by any means, electronic, mechanical, photocopying, recording or otherwise, without the prior written permission of the publisher, Elsevier Science Publishers B.V., Copyright & Permissions Department, P.O. Box 521, 1000 AM Amsterdam, The Netherlands.

Special regulations for readers in the U.S.A. – This publication has been registered with the Copyright Clearance Center Inc. (CCC), Salem, Massachusetts. Information can be obtained from the CCC about conditions under which photocopies of parts of this publication may be made in the U.S.A. All other copyright questions, including photocopying outside of the U.S.A., should be referred to the copyright owner, Elsevier Science Publishers B.V., unless otherwise specified.

No responsibility is assumed by the publisher for any injury and/or damage to persons or property as a matter of products liability, negligence or otherwise, or from any use or operation of any methods, products, instructions or ideas contained in the material herein.

This book is printed on acid-free paper.

Printed in The Netherlands.

# Spike Generation in Cortical Neurons: Probabilistic Threshold Function shows Intrinsic and Long-lasting Dynamics

Detlef Heck<sup>a</sup>, Stefan Rotter<sup>a</sup> and Ad Aertsen<sup>b 1</sup>

<sup>a</sup>Max-Planck-Institut für biologische Kybernetik, Spemannstraße 38, 7400 Tübingen,  
Germany

<sup>b</sup>Institut für Neuroinformatik, Ruhr-Universität, P.O.Box 10 21 48, 4630 Bochum,  
Germany

## Abstract

It is commonly assumed that action potentials are the means by which neurons transfer information and, hence, participate in computational and information processing tasks in the brain. Therefore, the rule that governs the generation of such action potentials (spikes) is one of the elementary principles in the nervous system. Generally, the occurrence of a spike is probabilistically related to the potential difference across the cell membrane, such that the firing probability increases with the trans-membrane potential; this dependence is usually described by the *neuronal threshold function*. Surprisingly, and in spite of its apparent importance, the detailed form of this threshold function for cortical neurons is still unknown. Therefore we decided to investigate this threshold firing in more detail on the basis of long intracellular recordings from cortical neurons *in vitro*. In order to quantify the results, we developed a statistical analysis procedure, specifically designed to capture the relevant dependences. This approach results in a *stochastic transfer function*, describing the dependence of the firing probability on the trans-membrane potential and on the time elapsed since the occurrence of that particular potential value. Our results indicate that this transfer function of cortical neurons shows intrinsic dynamic properties, which cannot be reduced to a single, instantaneous threshold function, as used in most theoretical descriptions and neural network models.

## 1. Introduction

Faced with the enormous complexity of the brain, expressed in the large number of different elements and their intricate electrical properties and interactions, it seems reasonable to seek to reduce this complexity by searching for general principles and to test their validity in experimental and theoretical models. Indeed, the invention of the computer and the corresponding enormous increase in computational power made the modelling of such complex systems a feasible enterprise. An important first step in this direction was made in 1943 by McCulloch and Pitts<sup>6</sup>, who reduced the known anatomical and physiological

<sup>1</sup>Additional support was received from the German Ministry for Science and Technology (BMFT)

variety of nerve cells to a simple binary threshold device, interacting with its neighbours via inhibitory and excitatory connections (the 'synapses'). This formal 'McCulloch-Pitts neuron' has only two activity states, and switches from the inactive to the active state when the sum over all inputs reaches a fixed threshold. Inhibition has a strong influence on a 'McCulloch and Pitts neuron', such that activity of only one inhibitory synapse fixes the 'neuron' in the inactive state (compare shunting inhibition). Although much has changed in our understanding of neural function since then, the notion of a neuron as a computational element with a nonlinear threshold function, transforming the input from many incoming fibers into a single output stream, remains common to most model formulations until the present day, irrespective of whether these models are continuous ('analog') neurons<sup>9</sup> or discrete ('spiking') neurons with 'action potential' events<sup>7</sup>.

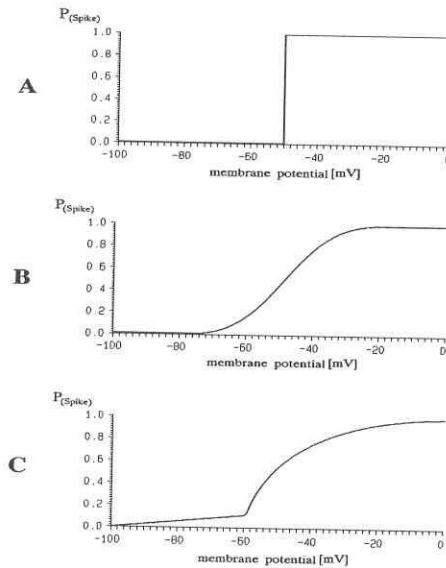


Figure 1: Three possible transfer functions for a single neuron model. A) A discrete threshold allows only two different output states. B) A sigmoid function defines a continuous mapping from the input to the output signal domain. C) A possible combination of A and B.

In many of these theoretical models, either one of two different types of threshold functions are assumed. One is the above mentioned 'hard', deterministic threshold proposed by McCulloch and Pitts<sup>6</sup> (Fig. 1A), the other is a 'soft', sigmoid shaped function introduced as a probabilistic descriptor by Little<sup>5</sup> (Fig. 1B)). Interestingly, and in spite of considerable early experimental work on peripheral nerves<sup>11</sup>, the detailed form of the threshold function of cortical neurons is still unknown. This is all the more surprising, considering that a number of studies, both theoretical and experimental, have repeatedly emphasized the functional importance of the nonlinear threshold of central neurons<sup>8,3</sup> (see also the contribution of Freeman in this Volume). Recently, the form of the threshold

function gave rise to a theoretical debate in the context of neural network models<sup>10</sup>. Here it was implicated in connection with the stability of neural activity, in particular at the low firing rates as typically observed in the neocortex<sup>1</sup>. In this context, an intermediate function was proposed<sup>4</sup>, combining the properties of the 'hard' and 'soft' threshold (Fig. 1C).

Inspired by these considerations, we set out to measure the detailed form of the firing threshold function of neocortical neurons under conditions of steady, low-level firing. To this end, we measured simultaneously the time course of the membrane potential and the events of spike occurrences by intracellular recording from spontaneously active cells in an acute slice preparation. In a subsequent stage, we carried out a specifically designed statistical analysis of the relation between the membrane potential value and the probability of observing a spike event. In this context, it soon became clear that it would not be possible to describe the firing probability as a function of membrane potential alone. Clearly, other variables such as the time that passed since a particular potential value was attained, are expected to have an influence too. The result of this analysis, which will be described below, is a *stochastic transfer function*, which, unlike the usual instantaneous firing threshold, expresses the firing probability as a function of the trans-membrane potential and of the time elapsed since that potential occurred.

## 2. Methods

Acute coronal slices (thickness 400  $\mu\text{m}$ ) were prepared from the visual cortex of 4 to 6 week old rats (Lewis) according to standard procedures, and kept at room temperature in an artificial cerebrospinal fluid (ACSF<sup>2</sup>). For the experiment, the slices were transferred to a recording chamber (temperature 33 to 36 °C), where they lay fully submerged on a glass cover slip. Intracellular recordings were made with glass micropipettes (3M potassium acetate) from cells in different layers of the cortical slice. The positions of the cells were estimated by visual inspection. If necessary, spontaneous spike activity of the cells was increased by adding 150 to 250  $\mu\text{M}$  l-Glutamate to the perfusion medium and/or by injection of a constant, depolarizing DC-current.

Intracellularly recorded signals were digitized at a sampling rate of 10 kHz using a CED 1401 (CED, Cambridge, UK) laboratory interface and written to disk for later processing.

## 3. Firing Threshold as a Probability Distribution

The intracellularly recorded signals were analyzed off-line. First, from the digitized signal we extracted the times of spike events as the instants of the spike waveform maxima (Fig. 2A). From these we could easily compute the usual spike statistics, such as the interval distribution (Fig. 2B) and the autocorrelation function (Fig. 2C). These provide information about the firing mode of the cell (e.g. stochastic or quasi-periodic), as is illustrated for a typical recording from a cortical cell in Fig. 2. For the period this particular cell fired in a stochastic mode, more or less like a Poisson process with dead-time, as can be inferred from the exponential-like interval distribution and the more or less constant autocorrelation. In other cases, the firing pattern could be more regular, up to the point of being (quasi-)periodic.

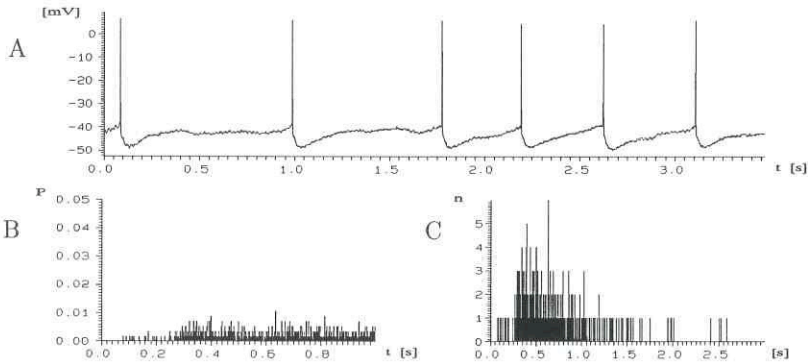


Figure 2: Typical segment of an intracellular recording from a cortical neuron in vitro (A), the autocorrelation function (B), and its interval distribution (C). This cell was recorded in layer II/III; a steady level of firing (mean inter-spike interval 638 ms, standard deviation 416 ms) was obtained by constant intracellular current injection (0.25 nA) and an addition of 200  $\mu$ M glutamate to the medium. A total number of 548 spikes was collected during a total analyzed time of 350 sec. Observe that the firing of this cell is very reminiscent of a Poisson process with dead-time (refractoriness).

The probability of spike generation as a function of membrane potential and time was investigated by making the following analysis: First, every occurrence of a certain value of the membrane potential  $\varphi_i$  was registered and counted; this results in the count  $n(\varphi_i)$  for that particular value. The collection of counts for all relevant values of  $\varphi$  is the potential distribution  $n(\varphi)$ . Second, whenever a particular membrane potential was found, we regarded this moment as time zero and determined the following two time intervals:

- 1)  $\tau^-$  : the time elapsed since the last spike,
- 2)  $\tau^+$  : the time to go until the next spike,

for  $\tau \leq$  some maximum value (in our application the duration of the longest inter-spike interval. See Fig. 3A.)

These two intervals were entered into two associated matrices of counts  $n(\tau^-, \varphi)$  and  $n(\tau^+, \varphi)$ , with the rows representing the potential values  $\varphi$  and the columns representing the different time values  $\tau$ . For each pair of doublets  $(\tau^-, \varphi)$  and  $(\tau^+, \varphi)$  found, the two corresponding matrix elements were incremented by one. This is illustrated in Figs. 3A,B, with the two members of each pair represented by the same symbol. The result of collecting all these pairs for all membrane potential values in the recording is two matrix histograms of counts, specifying for each potential value  $\varphi$  how often it was preceded by a spike at  $\tau^-$  ms, and how often it was followed by a spike at  $\tau^+$  ms.

From these matrix histograms we computed the transfer function of the neuron in terms of the firing probability as a function of membrane potential and time. It gives the probability of a spike  $Z$  to occur  $\tau^+$  milliseconds after the membrane potential attained

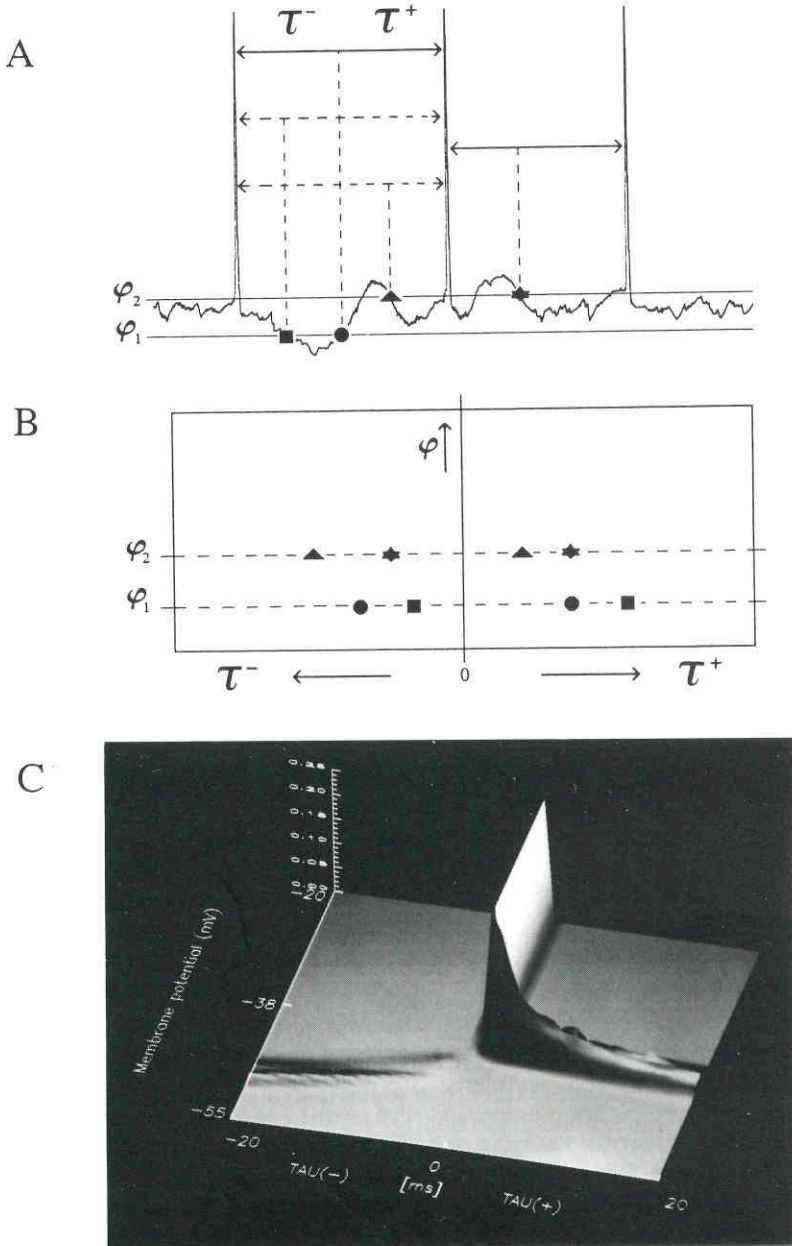


Figure 3: Illustration of the analysis procedure (A,B), and the resulting neural transfer function (C) for the cortical cell shown in Fig. 2. Further explanation see text.



a certain value  $\varphi$  (cf. the right-hand part of Fig. 3C).

$$P(Z^+ \text{ at } \tau^+ | \varphi) = \frac{n(\tau^+, \varphi)}{n(\varphi)} \quad (1)$$

The analogous procedure for  $\tau^-$  yields the probability of a spike  $Z$  to occur  $\tau^-$  milliseconds before a certain value  $\varphi$  of the membrane potential (corresponding to the left-hand part of Fig. 3C).

$$P(Z^- \text{ at } \tau^- | \varphi) = \frac{n(\tau^-, \varphi)}{n(\varphi)} \quad (2)$$

The graphical display of these probabilities is, consequently, a 3-dimensional graph with the firing probability plotted along the vertical axis, and membrane potential and time along the two horizontal axes. The two separate probabilities for  $\tau^-$  and  $\tau^+$  can be combined into a single one:  $P(Z^- \text{ at } \tau^-, Z^+ \text{ at } \tau^+ | \varphi)$ . This can be plotted in a single picture, with the time running along the x-axis, and time zero, i.e. the time when the potential value occurred, in the middle (Fig. 3C).

The result of this procedure for the recording from the neuron in Fig. 2 is shown in Fig. 3C. Observe that, surprisingly, the spike probability distribution for this cortical cell is a non-separable function of  $\varphi$  and  $\tau$ , covering a considerable region of the  $(\tau, \varphi)$ -space, with an elongated tail extending to high values of  $\tau$ . This result, which is quite typical for our recordings, is clearly in contrast to what should be expected for a neuron with a fluctuating membrane potential and an instantaneous threshold for spiking: in that case the probability distribution would essentially depend only on  $\varphi$  within a narrow range of  $\tau$ -values immediately adjacent to the origin. The consequences of this will be described in more detail below.

#### 4. The Influence of Membrane Potential and Time

In order to relate the above determined probability distribution to more conventional measures of the likelihood of spiking, we studied the behavior of the 'mountain range' in Fig. 3C at appropriately chosen cross-sections. This enables to further quantify the influence of each of the two variables  $\varphi$  and  $\tau$  separately, keeping in mind of course the observed non-separability of these respective influences. (This is, in fact, the reason why we have to resort to cross-sections, rather than to the marginal distributions, which could be obtained simply by appropriate projection.)

##### 4.1. Time-Dependent Threshold Functions

Let us first consider the influence of the membrane potential  $\varphi$ . This is, in fact, closely related to the original question on the form of the threshold function (cf. Fig. 1). Clearly, the 3-dimensional plot in Fig. 3C can be thought of to consist of a sequence of different threshold functions, each one referring to a different time  $\tau^+$  relative to the occurrence of a membrane potential. One can, for example, cut out a narrow slice, say 1 ms wide, from the 3-D probability distribution and, thus, arrive at the neural transfer function at time delay  $\tau$ :  $P(Z^+ \text{ at } (\tau^+ = \tau \text{ to } \tau + 1 \text{ ms}) | \varphi)$ .

Results of this procedure for three different choices of  $\tau$  (at 0, 2, and 4 ms) are shown in Fig. 4. Not surprisingly, in view of the result in Fig. 3C, we observe that the firing probability is far from being instantaneous. Apart from the immediate response (Fig. 4A), considerable contributions arise for larger time delays (Figs. 4B,C). In fact, extending our analysis beyond the time window of 20 ms (Fig. 3C), we found that distinct nonuniformities in the probability curves in these time slices continue to exist (albeit gradually diminishing as compared to those in Figs. 4B,C) for delays of up to 200 ms or even more! This results obviously in a considerable amount of irregularity in the timing of spikes, to which we will return in the next section. Each of the threshold curves in Fig. 4 is characterized by a relatively smooth onset. The question whether this results from an intrinsically smooth threshold, or rather from a discrete, but fluctuating threshold that becomes blurred by the time averaging inherent to our analysis, cannot be decided at this point. Only the instantaneous response (Fig. 4A) shows saturation at probability one for high values of the membrane potential; curves at later times decrease again for increasing  $\varphi$  (Figs. 4B,C), reflecting refractoriness due to firing in earlier time intervals. Finally, there is a distinct tendency of the onset potential in the threshold curves to decrease with increasing time delay. This decrease saturates in the course of the first 5 ms, after which the threshold curves remain essentially the same, both in position and form, with only the amplitude very slowly decaying in the course of the ensuing few hundred milliseconds.

#### 4.2. Voltage-Dependent Spike Latency Statistics

Another perspective on the spike probability distribution can be gained from choosing the orthogonal point of view. Making a cross-section along the  $\tau$ -axis of Fig. 3C yields the distribution of spike latencies, relative to the time of occurrence of a particular membrane potential. A useful and compact way to characterize such a latency distribution is to specify its moments. Hence, we calculated for each delay distribution the first two moments - the mean latency and the standard deviation - and plotted these as a function of the membrane potential.

In addition, we calculated from them the coefficient of variation  $cv = \frac{\text{std.dev.}}{\text{mean}}$ ; this is a commonly used measure in spike statistics which, roughly speaking, measures the departure from an exponential distribution for which  $cv=1$ .

The resulting statistics for our cortical cell are shown in Fig. 4 (bottom row). Observe that the mean latency (Fig. 4D) and the standard deviation (Fig. 4E) show a distinct and similar dependence on membrane potential. They both start at low values around  $\varphi = -35$  mV, gradually increase when the membrane potential becomes more negative, to attain extremely high values (up to 500 ms) around  $-46$  mV. Both curves show a non-monotonicity for more negative potentials, for which we currently have no explanation. One possibility might be that this reflects certain properties of voltage-dependent ion channels.

Roughly speaking, these results imply that for more negative membrane potentials, spikes tend to occur both later and less precise in time. The relation between the two is expressed in their ratio, the coefficient of variation (Fig. 4C). Starting off closely above 1 at  $-38$  mV, it rapidly rises to a peak of 3.4 at about  $-40$  mV, after which it monotonically decays to a constant value around 0.7 for membrane potential values below about  $-47$  mV. Interestingly, for much of the range of membrane potential values the coefficient

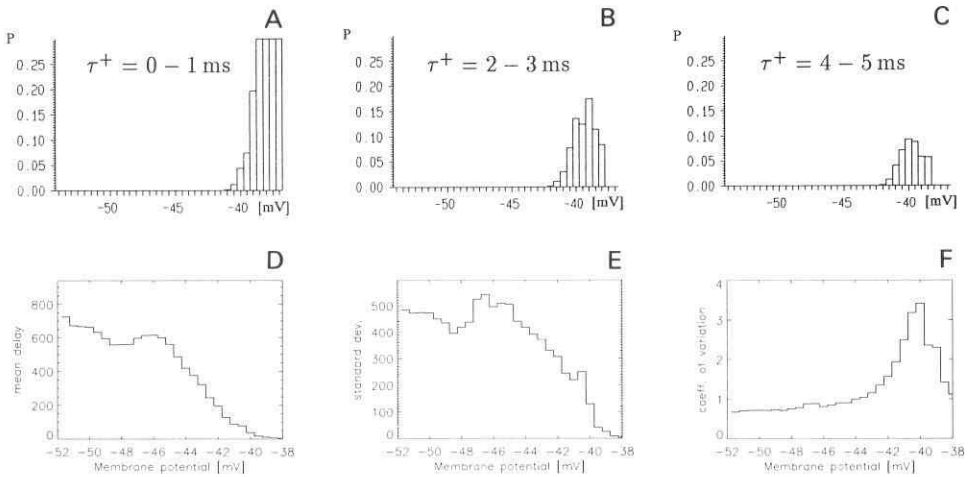


Figure 4: Firing probability functions (top row) and spike latency statistics (bottom row). Data are from the same cortical cell as in Figs. 2 and 3. Top row: Firing probability as a function of membrane potential for different time delays after that potential occurred: 0-1 ms (A), 2-3 ms (B), and 4-5 ms (C). Bottom row: Mean delay (D), standard deviation (E), and coefficient of variation (F) of the spike latency distribution.

of variation is 1 or higher. This implies that throughout this range, i.e. even for membrane potentials with a very high probability of firing, there is always an uncertainty as to when the spike will actually occur, which roughly equals the mean latency or is even higher. The result of this is evidently a considerable degree of stochasticity, as is confirmed by the spike train's Poisson-like behavior (cf. Fig. 2; see also the contribution of Rotter et al., this volume). The sharp peak in the relative uncertainty (Fig. 4F) seems to be primarily caused by a concurrent increase in the standard deviation (Fig. 4E), whereas the mean delay continues its smooth course in the corresponding potential regime (Fig. 4D). Apparently, there is a narrow voltage range (say, between  $-39$  and  $-42$  mV in which firing is distinctly less precise in time than outside this range.

## 5. Discussion

We determined the stochastic neural transfer function of cortical neurons in vitro by statistical analysis of intracellularly recorded membrane potentials and spike sequences. This transfer function specifies the probability  $P(Z^+ \text{ at } \tau^+ | \varphi)$  for the generation of a spike some time  $\tau^+$  after a certain membrane potential  $\varphi$  occurred. Appropriate cross-sections of this probability distribution can be related to conventional threshold curves and spike latency statistics.

We found that different cortical cells may have different transfer functions. This is expressed in the different shapes of the 3-dimensional probability distributions and, accordingly, in the different sets of threshold functions and spike latency statistics. However,

one important feature shared by all cortical cells is that the neural transfer function is generally a non-separable function of membrane potential and time, extending over a varying, but in each case considerable region of the  $(\varphi, \tau)$ -space. Consequently, single cortical neurons are expected to exhibit a considerable degree of randomness in the timing of their individual spike firings.

Occasionally we encountered neurons which, during the recording, switched spontaneously from a stochastic to a periodic firing mode, presumably related to small changes in the baseline membrane potential. Separate analysis of these different modes revealed drastically different transfer functions. Thus, cortical neurons may have different modes of firing, with each mode having its own specific transfer function.

In summary, our findings indicate that the transfer function of cortical neurons shows intrinsic dynamic properties. The non-separability of the different dependences implies that the transfer function cannot be reduced to a single, instantaneous threshold function, as used in most theoretical descriptions and neural network models.

## References

1. M. Abeles et al., Firing patterns of single units in the prefrontal cortex and neural network models, *Network*, 1 (1990) 13.
2. L. J. Bindman et al., Comparison of the electrical properties of neocortical neurones in slices in vitro and in the anaesthetized rat, *Exp. Brain Res.*, 69 (1988) 489.
3. F. H. Eeckman and W. J. Freeman, Asymmetric sigmoid non-linearity in the rat olfactory system, *Brain Res.*, 557 (1991) 13
4. D. Kleinfeld and H. Sompolinsky, in: C. Koch and I. Segev, eds., *Methods in neuronal modeling. From synapses to networks*, MIT Press (1989)
5. W. A. Little, The existence of persistent states in the brain, *Math. Biosci.*, 19 (1974) 101.
6. W. S. McCulloch and W. Pitts, A logical calculus of the ideas immanent in nervous activity, *Bull. Math. Biophys.*, 5 (1943) 115
7. N. Rochester et al., Tests on a cell assembly theory of the action of the brain, using a large digital computer, *IRE Trans. Inform. Theory*, IT-2 (1956) 80.
8. T. Sejnowski, in: G. E. Hinton and J. A. Anderson, eds., *Parallel models of associative memory*, (Lawrence Erlbaum Assoc., Hillsdale, New Jersey, 1981)
9. W. K. Taylor, Electrical simulation of some nervous system functional activities, *Information Theory*, Vol. 3 (ed. E. C. Cherry), (1956) 314, London: Butterworths.
10. G. Toulouse, Perspectives on neural network models and their relevance to neurobiology, *J. Phys. A: Math. Gen.*, 22 (1989) 1959.
11. A. A. Verveen, On the fluctuation of threshold of the nerve fiber, *Proc. 2nd Int. Meeting of Neurobiologists* (1959) 282.